Comparison of the MODIS Collection 5 Multilayer Cloud Detection Product with CALIPSO

Steven Platnick[a], Gala Wind[a], Michael D. King[b], Robert E. Holz[c], Steven A. Ackerman[c], and Fred W. Nagle[c]

[a]*Laboratory for Atmospheres, NASA Goddard Space Flight Center, Greenbelt, MD USA*
[b]*Laboratory for Atmospheric and Space Physics, University of Colorado, Boulder, CO USA*
[c]*Space Science and Engineering Center, University of Wisconsin, Madison, WI USA*

Abstract. CALIPSO, launched in June 2006, provides global active remote sensing measurements of clouds and aerosols that can be used for validation of a variety of passive imager retrievals derived from instruments flying on the Aqua spacecraft and other A-Train platforms. The most recent processing effort for the MODIS Atmosphere Team, referred to as the Collection 5 scream, includes a research-level multilayer cloud detection algorithm that uses both thermodynamic phase information derived from a combination of solar and thermal emission bands to discriminate layers of different phases, as well as true layer separation discrimination using a moderately absorbing water vapor band. The multilayer detection algorithm is designed to provide a means of assessing the applicability of 1D cloud models used in the MODIS cloud optical and microphysical product retrieval, which are generated at a 1 km resolution. Using pixel-level collocations of MODIS Aqua, CALIOP, we investigate the global performance of multilayer cloud detection algorithms (and thermodynamic phase).

INTRODUCTION

The Collection 5 MODIS cloud optical and microphysical properties data set includes a research-level product designed to detect those multilayer cloud scenes that can significantly affect microphysical retrievals of the predominant cloud layer in absorbing shortwave infrared spectral bands. The algorithm is primarily intended to flag layers of different thermodynamic phase, e.g., ice clouds overlying liquid water clouds, but is also sensitive to layers of a single phase separated by a significant water vapor absorption path in the 0.94 μm spectral region. Since retrievals are based on homogeneous cloud models, mixed phase signals can often cause cloud effective radius retrievals to be biased high for multilayer scenes retrieved as liquid phase, or biased low for ice phase retrievals. The multilayer flag allows microphysical retrievals to be screened prior to statistical analyses (e.g., MODIS Level-3 binned data).

To evaluate the performance of the MODIS multilayer cloud product, we have executed a series of overlapped cloud simulations using the DISORT radiative transfer code for different cloud layer separations, and atmospheric and surface conditions. The multilayer results have also been compared with results from CALIPSO active measurements (however those results were not available in time to be included in this extended abstract), which are collectively capable of discerning multiple cloud layers over much of the space of interest. The inclusion of CloudSat observations is pending. There are a number of questions investigated using the cloud simulations: How does the detection of multilayer clouds change with atmospheric conditions, in particular with changes in the column water vapor amount? What effect does surface albedo have on successful detection? How does detection change with layer separation and viewing geometry changes? In the following sections we show a sample of the simulation results.

RADIATIVE TRANSFER CALCULATIONS

In order to thoroughly test the performance of multilayer cloud detection algorithm we have set up an extensive set of cloud simulations to capture the algorithm behavior under a variety of conditions.

The cloud layers were specified as follows: a 1 km thick liquid water cloud was placed at altitudes of either 2 or 4 km, and an ice crystal cloud layer of 2 km thickness at an altitude close to the tropopause of the particular atmospheric profile used. Because the algorithm depends in part on water vapor absorption, realistic cloudy atmosphere profiles were needed. We generated our own cloudy atmospheric profiles from the European Center for Medium-range Weather Forecasts (ECMWF) ERA-40 (40-year reanalysis) atmospheric profile database averaged down to 36 vertical layers. Only profiles with high cloud fractions CF > 0.85 were used, i.e., the profile was selected for use if the cloud fraction in any vertical layer was greater than 85%. The selected profiles were then subdivided further by latitude and time of year to create cloudy mean mid-latitude summer (MLS) and winter (MLW), tropical (TRP), and polar (POL) profiles. The tropical belts were between ±30°, midlatitude between 30° and 60° of each hemisphere, and polar with latitudes poleward of 60°. The temporal separation was done using May 1st as the beginning of Northern hemisphere summer and November 1st as the beginning of Northern hemisphere winter (and reversed for Southern hemisphere). The profiles were also subdivided into land and ocean using the ECMWF land fraction flag with LF > 0.5 threshold indicating an over-land profile. The POL profiles were taken to be polar ocean only, i.e., the Antarctic continent has been excluded from the study. The resulting profiles were then saturated with respect to the appropriate thermodynamic phase in the layers of the atmosphere where the clouds were placed in the simulations as shown in Figure 1.

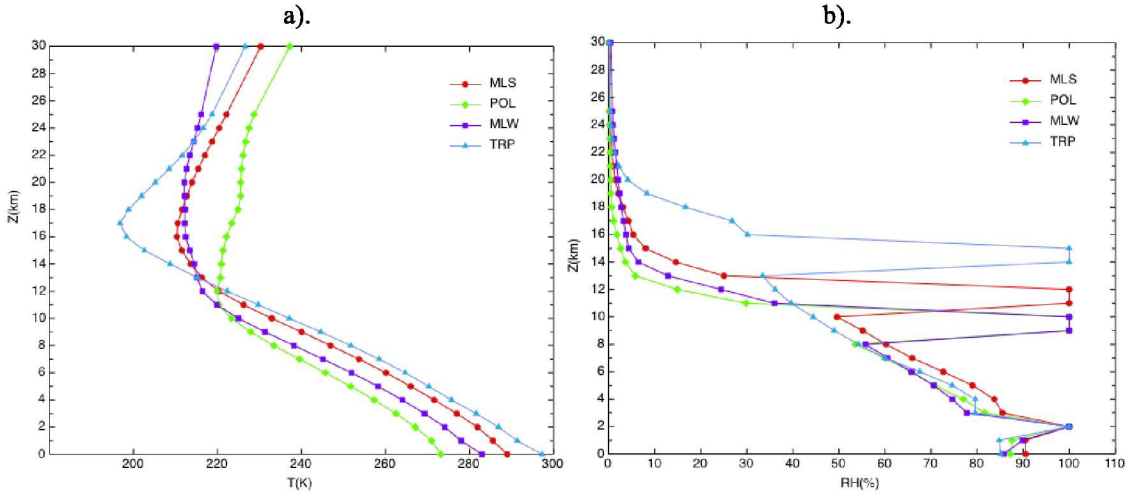

FIGURE 1. Plots of the average atmospheric profiles used in the simulations: a) temperature as a function of altitude for the first 30 km of the atmosphere, and b) relative humidity as a function of altitude. The example relative humidity profiles contain a liquid water cloud at a 2 km altitude and 2 km thick ice cloud layers near the tropopause of each profile.

The radiaitve transfer calculations were then performed using a selection of solar and view geometry appropriate for the latitude and time of year derived from the MODIS global monthly (MOD08_M3) product. The surface albedo data was taken from Moody et. al. (2005, 2007) [1,2] MOD43-based global 1 km albedo product. The calculations were performed for ice cloud effective particle radii of 10, 30 and 50 microns and water droplets of 6, 10 and 20 microns. A range of optical thicknesses for ice and liquid water clouds were used. The simulation results consisted of 26 files with 7560 data points each (a data point being a set of the 16 MODIS channels needed to perform the complete MODIS cloud optical and microphysical property retrieval algorithm, including the cloud top property retrieval using the CO_2 slicing technique for high clouds). The resulting input files were processed by the operational Collection 5 MODIS cloud retrieval code (version 5.12.4) [3].

SIMULATED RETRIEVALS AND RESULTS

The MODIS multilayer cloud detection algorithm uses a combination of tests, which include differences in above-cloud precipitable water retrievals using CO_2 slicing channels and model analyses versus a near-infrared (0.94 μm) water vapor band retrieval. Differences in retrieved shortwave infrared and infrared phase are also utilized as well as a number of thresholds to aid retrievals over bright surfaces.

A sample of the results contained in the database are shown in Figs. 2 and 3. Figure 2 shows multilayer cloud detection results as a function of atmospheric moisture content. This is a slice through the database for nadir view and a 23° solar zenith angle. The cloud effective radii are 30 microns for ice and 10 microns for liquid water. The liquid water cloud is at 2 km altitude. A Lambertian ocean surface albedo is set at 0.05, i.e., diffuse illumination conditions are assumed. The legend indicates the combination of cloudy profiles that trigger a positive multilayer flag as a function of ice and water cloud optical thickness. This shows the moisture dependence of the detection algorithm. More moist atmospheres become sensitive to presence of thinner cirrus, but lose sensitivity quicker as the ice cloud gets optically thicker. Note that there are no false positives and a wide range of ice cloud optical thickness for which multilayer detection is possible for all atmospheres ($0.5 \leq \tau_{ice} \leq 8$ for optically thick water clouds).

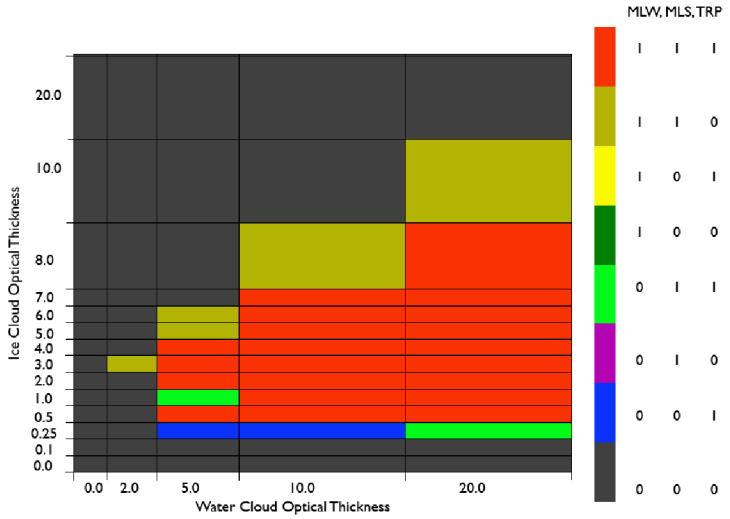

FIGURE 2. Multilayer cloud detection results as a function of atmospheric moisture content over an ocean surface. Combinations of MLW, MLS, and TRP cloudy atmosphere profiles are shown on the legend.

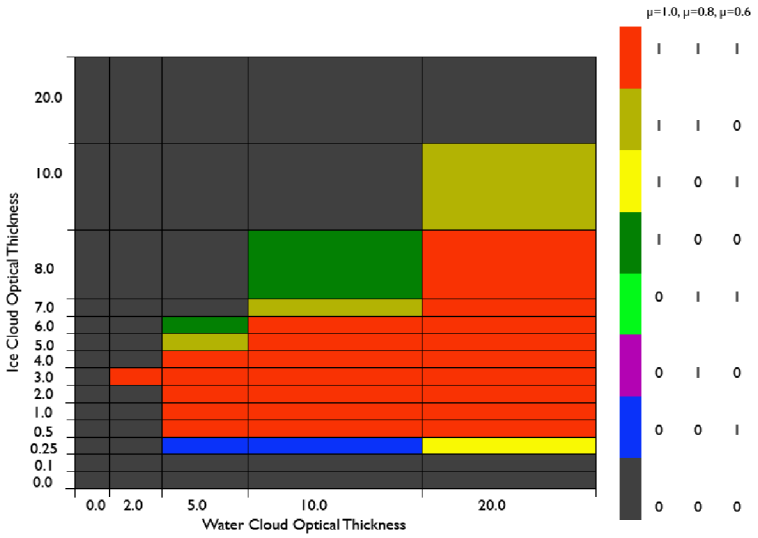

FIGURE 3. Multilayer cloud detection results as a function of view geometry over an ocean surface.

Figure 3 shows the combination of view zenith angles that trigger a positive flag result, and thus represents the dependence of the algorithm on view angle. The solar zenith angle was held constant at 23° with relative azimuth at 0°. Results are for an ocean surface, a cloudy MLS atmosphere, and a liquid water cloud at 2 km. Thinner cirrus gets flagged at more oblique view angles, but the sensitivity is retained for thicker clouds at more direct view angles.

COMPARISONS WITH CALIPSO

Operational results from the MODIS multilayer cloud detection algorithm applied to Aqua MODIS have been compared with results from the CALIPSO CALIOP lidar, which can detect the presence of a subset of multilayer clouds by direct measurement. Screening by CALIOP upper-level cloud optical thickness is being investigated; cirrus optical thickness is determined from extinction in individual layers that are retrieved at a minimum 5 km average of individual laser shots. We have defined a multilayer cloud if there is at least 3 km vertical layer separation in the CALIOP layer identification product. MODIS multilayer cloud product is a 1 km product and so comparisons are done using the maximum value of the multilayer cloud flag within a 5 km CALIOP track. This study is ongoing.

CONCLUSIONS AND FUTURE WORK

The DISORT simulations of multilayer clouds show some of the strengths and also some of the sensitivities of the MODIS multilayer cloud detection algorithm. There is some dependence on the amount of column water vapor as well as the view geometry. We plan on performing more examination of the result dataset to retrieve even more information about the retrieval performance. Comparisons with CALIPSO look favorable with a significant amount of agreement between the two methods despite the comparison method of CALIPSO averaging to 5km.

In addition to further CALIPSO analysis and inclusion of CloudSat observations, plans include comparisons against other multilayer cloud studies. These include the Niu, et.al. [4] infrared calculations, the Nasiri et.al. [5] multispectral multilayer cloud detection algorithm, and the Pavolonis and Heidinger [6] algorithm for AVHRR and VIIRS spectral bands.

ACKNOWLEDGMENTS

This work was performed with support from the NASA Radiation Sciences Program.

REFERENCES

1. Moody, E. G., M. D. King, S. Platnick, C. B. Schaaf, F. Gao, 2005: Spatially complete global spectral surface albedos: Value-added datasets derived from Terra MODIS land products. *IEEE Trans. Geosci. Remote Sens.*, **43**, 144-158.

2. Moody, E. G., M. D. King, C. B. Schaaf, D. K. Hall, and S. Platnick, 2007: Northern Hemisphere five-year average (2000-2004) spectral albedos of surfaces in the presence of snow: Statistics computed from Terra MODIS land products. *Remote Sens. Environ.*, 111, 337-345..

3. MODIS Cloud Optical and Microphysical Properties (MOD06) Collection 5 change document: http://modis-atmos.gsfc.nasa.gov/products_C005update.html.

4. Niu, J., P. Yang, H. L. Huang, J. E. Davies, J. Li, B. A. Baum, and Y. X. Hu, 2007: A fast infrared radiative transfer model for overlapping clouds. *J. Quant. Spectrosc. Radiant. Transfer*, Vol. 103, 447-459.

5. Nasiri, S. L. and B. A. Baum, 2004: Daytime multilayered cloud detection using multispectral imager data. *J. Atmos. Ocean. Technol.*, 21, 1145-1155.

6. Pavolonis, M. J. and Heidinger, A. K.. Daytime cloud overlap detection from AVHRR and VIIRS. *Journal of Applied Meteorology*, Volume 43, Issue 5, 2004, pp.762-778.